# Investigation of heavy particle radioactivity and spontaneous fission of even Z superheavy nuclei*

Kirandeep Sandhu[1] Gurjit Kaur[2†] Manoj K. Sharma[2]

[1]P.G. Department of Physics, G.S.S.D.G.S Khalsa College Patiala, Punjab, India
[2]Department of Physics and Materials Science, Thapar Institute of Engineering and Technology, Patiala - 147004, Punjab, India

**Abstract:** The Preformed Cluster Model (PCM) is applied to investigate the heavy particle radioactivity (HPR) and spontaneous fission (SF) processes for even-Z superheavy nuclear systems. Different proximity potentials are used to calculate decay half-lives of Z=112-120 nuclei. The fragmentation potential and preformation distribution suggest that spontaneous fission is the major contributor upto Z=114 and HPR starts competing for heavier nuclei. The heavy cluster emission is supported by Pb-magicity whereas SF is reinforced due to the deformations of fission fragments. The heavy cluster decay half-lives ($Log_{10}T_C$) are calculated using PCM and are compared with the estimates of Analytical Super Asymmetric Fission (ASAF) Model. The calculated $Log_{10}T_C$ show nice agreement with the ASAF measurements for the use of Prox-00 and Mod Prox-00 versions of potentials. However, Prox-77, Prox-88, and Prox-BW-91 are not appropriate to address the $Log_{10}T_C$ for Z≥116 nuclei. In order to resolve this, Z-dependence in the radius parameters is included. Interestingly, half-lives match the ASAF data after the inclusion of Z-dependence. The branching ratios are also calculated for superheavy nuclei and compared with the estimates of Unified description (UD) formula, Universal (UNIV) curve, Universal decay law (UDL), Horoi formula and ASAF measurements. Further, the spontaneous fission half-lives ($T_{SF}$) of $^{282}$Cn, $^{284}$Cn, $^{284}$Fl and $^{286}$Fl superheavy nuclei are also estimated through various proximity potentials. Among all, Prox-00 is appropriate to address the experimental data nicely. Using same, the spontaneous fission half-lives are estimated through PCM for Z=116-120 isotopes at different neck-length parameters. Finally, the scaled total kinetic energy (TKE) values are compared nicely with the available data.

**Keywords:** Heavy Particle Radioactivity, Preformed Cluster Model, Ground State Decay

**DOI:** **CSTR:**



## I. INTRODUCTION

In ground state, the unstable nuclear system attains stability either by expelling ionized particles or radiations. Owing to this, three principle decay processes fall in this category namely alpha ($\alpha$), beta ($\beta$) and gamma ($\gamma$) emissions. However, apart from these decay channels the cluster (or heavy cluster) radioactivity and spontaneous fission are equally important to investigate the ground state dynamics of heavy and superheavy elements. Among these, spontaneous fission find its genesis while investigating the decay of $^{235}$U nucleus into two comparable fragments after capturing a neutron [1]. The division of nucleus into two massive parts was named as nuclear fission. The study had opened a new window for nuclear physicists to observe unstable heavy and superheavy nuclei through spontaneous fission process. In particular, for the superheavy mass region the probability of fission is paramount due to high Coulomb repulsion, hence $Z^2/A$ factor plays an important role for the segregation of fission fragments. Moreover, the magicity at Z=114,120,126 and N=172,184 magic shells is another milestone for investigating fission barriers for superheavy nuclei. Precisely, the calculated shell correction energies at superheavy magic shells provide stability against prompt fission and further help in investigating the island of stability [2, 3]. This signifies the importance of interplay between shell effects and Coulomb repulsion for SF process. Even and odd nucleons also influence the spontaneous fission events. In odd nuclear systems, strong hinderance is caused by an unpaired nucleon towards fission process [4]. Conclusively, the ground state fission which usually dominates in 108≤Z≤114 and 170≤N≤180 mass region is effected by various parameters which should be accounted while investigating its dynamics [5, 6]. Owing to this, the Preformed Cluster Mod-

Received 14 August 2024; Accepted 19 December 2024

* This work is supported by the Department of Science and Technology (DST) and Science and Engineering Research Board (SERB), New Delhi (File no. CRG/2021/001144)

† E-mail: kaursaini2505@gmail.com

el (PCM) [7−12] is applied in present analysis to study the SF half-lives ($T_{SF}$) of Z=112 and Z=114 isotopes. The shell effects of the parent nuclei and fissioning fragments are duly incorporated alongwith the liquid drop potential. In addition to this, the deformation effects are included upto $\beta_{2i}$ within the hot optimum orientation approach [13]. Moreover, role of different versions of proximity potentials namely Prox-77 [14], Prox-00 [15], Mod Prox-00 [16], Prox-88 [17] and Prox BW-91 [17] is tested for calculating $T_{SF}$ of Z=112 and 114 nuclear systems.

The ground state decay mechanism for Z≥114 is immensely effected by doubly magic $^{208}$Pb nucleus; leading to the emission of exotic clusters with $Z_{cluster}$>28. This process is coined as heavy particle radioactivity (HPR) [12, 18, 19]. Broadly speaking, the decay phenomenon lying between $\alpha$-emission and spontaneous fission events is termed as cluster (or heavy particle) radioactivity. It is relevant to mention that the peculiar decay mode was first investigated for trans-lead nuclei with Z = 87-96. The emission of $^{14}$C, $^{20}$O, $^{23}$F, $^{22,24-26}$Ne clusters [20−22] is mainly observed in this mass region. Subsequently, Poenaru *et.al.* [18, 19] has extended the work for superheavy nuclei with $Z_{parent}$>110 through Analytic Super Asymmetric Fission Model (ASAF). Various methodologies such as Unified fission model (UFM) [23−25], Generalized liquid drop model (GLDM) [26, 27], Universal decay law (UDL) [28, 29], Density dependent cluster model [30], Universal Curve (UNIV) [31], Unified description (UD) formula [32], Fission-based semi-empirical formula (semFIS) [33], and AKRA (from the Author Akrawy) [34] were then fabricated to address the heavy cluster emission. Among the mentioned methodologies, PCM follow approach where the clusters are assumed to be preformed inside the parent nucleus with finite value of preformation factor ($P_0$). The preformation probability ($P_0$) is calculated by solving the Schrodinger equation for the dynamic flow of charges and masses [35−37]. Afterwards, the cluster in the parent nucleus are presumed to penetrate with available Q-value through the interaction barrier. Opting the same, PCM is applied in the present work to understand the heavy particle radioactivity (HPR) of Z=112-120 nuclear systems in terms of preformation factor and penetration probability of clusters. It is relevant to mention that the Santhosh *et. al.* [38] has addressed the ASAF data [39] by calculating $\alpha$-decay and heavy cluster decay probabilities of superheavy isotopes. However, the present analysis through PCM mainly concentrates on following points:

(1) The main aim of this work is to test the effect of different proximity potentials namely Prox-77 [14], Prox-00 [15], Mod Prox-00 [16], Prox-88 [17], and Prox BW-91 [17], on heavy cluster emission and spontaneous fission from even-Z superheavy nuclei.

(2) The role of Z-dependent radius [40] in various proximity potentials is investigated to address both phenomenon.

The paper is organized as follows: the methodology in Section II, includes the framework of Preformed Cluster Model (PCM). Various versions of the proximity potentials are also briefed. Calculations and results are discussed in section III and finally the outcomes are summarized in section IV.

## II. METHODOLOGY

The Preformed Cluster Model (PCM) [7−12] based on Quantum Mechanical Fragmentation Theory (QMFT) [41, 42] has been developed by opting the Gamow's theory for penetration of the emitted particles/fragments. Here, instead of a square well or harmonic potential a more realistic nuclear proximity potential is included in the present work. Using different versions of proximity potentials (mentioned in subsequent work) the spontaneous fission and cluster emission half-lives are calculated by including: cluster and daughter preformation probabilities ($P_0$), barrier impinging frequency ($f_0$), and barrier penetrability (P), which are calculated as:

$$\lambda^{PCM} = f_0 P P_0,\ T_{\frac{1}{2}} = \frac{\ell n 2}{\lambda} \tag{1}$$

Here $P_0$ and P refer respectively to the $\eta$ and R motions of the fragments, and the third factor of Eq. (1) can be calculated as:

$$f_0 = \frac{(2E_2/\mu)^{1/2}}{R_0} \tag{2}$$

Here $f_0$ is depicted as the impinging or assault frequency of cluster where $R_0$ is the radius of parent nucleus. The impinging frequency $f_0$ is nearly constant $\sim 10^{21} s^{-1}$ for cluster and spontaneous fission processes.

Within the quantum mechanical fragmentation theory, the preformation probability $P_0$ is calculated by solving the Schrödinger equation, and the potential required for this mechanism is called the fragmentation potential $V_R(\eta)$ which is calculated as:

$$V(\eta,R) = -\sum_{i=1}^{2} B_i(A_i,Z_i) + V_c(R,Z_i,\beta_{\lambda i},\theta_i) + V_p(R,A_i,\beta_{\lambda i},\theta_i) \tag{3}$$

Here, binding energies of the two fragments, $B_i(i=1,2)$, are obtained using Audi and Wapstra's experimental compilation [43] and from the theoretical estimates of Möller *et.al.* [44]. The Möller-Nix *et. al.* binding energies are included for those nuclear systems which are absent in [43]. The binding energies are essentially the

sum of the liquid drop component $V_{LDM}$ and $\delta$U (empirical shell corrections [45]). The second term reflects Coulomb interaction and $V_P$ is the nuclear proximity potential. In this work different versions of proximity potentials are used namely Prox-77, Prox-00, Mod Prox-00, Prox-88, and Prox BW-91. A brief account of these potentials is given below:

**(a) Proximity-1977 (Prox-77):** The Prox-77 is based on the pocket formula of Blocki [14], and is calculated as the product of surface constant, universal function and mean curvature radius:

$$V_P = 4\pi\gamma b\bar{R}\Phi(s_0)MeV \tag{4}$$

Here mean curvature radius ($\bar{R}$) is:

$$\bar{R} = \frac{C_1C_2}{C_1+C_2} \tag{5}$$

with

$$C_i = R_i\left[1-\left(\frac{b}{R_i}\right)^2+.....\right] \tag{6}$$

and

$$R_i = 1.28A_i^{1/3}-0.76+0.8A_i^{-1/3}fm \tag{7}$$

The universal function is parameterized as:

$$\Phi(s_0) = \begin{cases} -\frac{1}{2}(s_0-2.54)^2-0.0852(s_0-2.54)^3 \\ -3.437\exp(-\frac{s_0}{0.75}) \end{cases} \tag{8}$$

respectively, for $s_0 \le 1.2511$ and $s_0 \ge 1.2511$.

The surface energy constant used for this potential is calculated as:

$$\gamma = 0.9517\left[1-1.7826\left(\frac{N-Z}{A}\right)^2\right]MeVfm^{-2}. \tag{9}$$

Here, $N$ and $Z$ are the total neutrons and protons of the considered nuclear system.

**(b) Proximity-1988 (Prox-88):** In Prox-88 [17], the $\gamma$ term was modified and the revised surface energy constant is given by

$$\gamma = 1.2496\left[1-2.3\left(\frac{N-Z}{A}\right)^2\right]MeVfm^{-2}. \tag{10}$$

**(c) Proximity-2000 (Prox-00):** In this version of proximity potential, the universal function is taken from Myers and Swiatecki [15], which reads as:

$$\Phi(s_0) = \begin{cases} -0.1353+\sum_{n=0}^{5}[c_n/(n+1)](2.5-s_0)^{n+1} \\ \quad \text{for} \quad 0 < s_0 \le 2.5, \\ -0.09551\exp[(2.75-s_0)/0.7176] \\ \quad \text{for} \quad s_0 \ge 2.5. \end{cases} \tag{11}$$

The nuclear charge radius is included in Prox-00 which is calculated as:

$$R_{00i} = 1.240A_i^{1/3}\left[1+\frac{1.646}{A_i}-0.191\left(\frac{A_i-2Z_i}{A_i}\right)\right]fm. \tag{12}$$

The surface energy constant used for this potential is

$$\gamma = \frac{1}{4\pi r_0^2}\left[18.63(MeV)-Q\left(\frac{t_1^2+t_2^2}{2r_0^2}\right)\right]MeVfm^{-2}. \tag{13}$$

For further details of coefficients see Ref. [15, 46].

**(d) Modified Prox-2000 (Mod Prox-00):** In this version of potential [16] nuclear charge radius is slightly different from the one used earlier in Prox-00 and is given by:

$$R_{00i} = 1.2332A_i^{1/3}\left[1+\frac{2.348443}{A_i}-0.151541\left(\frac{A_i-2Z_i}{A_i}\right)\right]fm. \tag{14}$$

**(e) Proximity BW-91 (Prox BW-91):** The proximity potential [17] is written as:

$$V_P = -\frac{V_0}{1+exp(\frac{r-R_0}{0.63})} \tag{15}$$

with

$$V_0 = 16\pi\gamma a\frac{R_1R_2}{R_1+R_2} \tag{16}$$

Here a=0.63 fm, $R_0$=$R_1$+$R_2$+0.29, and $R_i$ is defined as

$$R_i = 1.233A_i^{1/3}-0.98A_i^{-1/3}fm \tag{17}$$

The surface energy constant used for this potential is

$$\gamma = 0.95\left[1-1.8\left(\frac{N_P-Z_P}{A_P}\right)\left(\frac{N_t-Z_t}{A_t}\right)\right]MeVfm^{-2}. \tag{18}$$

The Coulomb potential [47, 48] for two charge fragments is given by

$$V_C(R,Z_i,\beta_{\lambda i},\theta_i,T) = \frac{Z_1Z_2e^2}{R} + 3Z_1Z_2e^2 \times \sum_{\lambda,i=1,2} \frac{R_i^{\lambda}(\alpha_i)}{(2\lambda+1)R^{\lambda+1}} \times Y_{\lambda}^{(0)}(\theta_i)\left[\beta_{\lambda i} + \frac{4}{7}\beta_{\lambda i}^2 Y_{\lambda}^{(0)}(\theta_i)\right] \quad (19)$$

Here, $Y_{\lambda}^{(0)}(\theta_i)$ is the spherical harmonic function and deformations $\beta_{\lambda i}$ (we use $\beta_{2i}$ alone) are taken from Ref. [44].

In literature the role of dynamic deformations of cluster and residual nuclei are discussed in [49, 50] where the nuclear shape parametrization depends on several dynamical degrees of freedom. On the other hand, in PCM [7−12] the Schrödinger equation is solved as a function of mass-asymmetry parameter $\eta$=(A1-A2)/(A1+A2), so as to obtain the relative formation probability of the most probable fragments in the exit channel. As the relative probability of all fragments of exit channel is required in the collective clusterization process adopted in PCM so use of dynamical deformations make the task very complex. Therefore static deformations are used in the present analysis.

The stationary Schrödinger equation for motion at fixed R-value reads as

$$\left\{-\frac{\hbar^2}{2\sqrt{B_{\eta\eta}}}\frac{\partial}{\partial\eta}\frac{1}{\sqrt{B_{\eta\eta}}}\frac{\partial}{\partial\eta} + V(\eta)\right\}\psi^{\nu}(\eta) = E^{\nu}\psi^{\nu}(\eta) \quad (20)$$

The mass parameters, ($B_{\eta\eta}(\eta)$) are the conventional hydrodynamical masses of Kröger and Scheid [51]. For cluster emission and other ground state decay processes, only the ground state ($\nu$=0) solution is relevant. The first turning point is therefore reached with the normalized fractional cluster preformation probability $P_0$ at a fixed R (=$R_a$) and is calculated as:

$$P_0 = |\psi(\eta(A_i))|^2 \sqrt{B_{\eta\eta}}\frac{2}{A} \quad (21)$$

Instead of calculating the radial Schrödinger equation for R motion, the penetration probability P is determined using the WKB approximation.

$$P = P_a W_i P_b \quad (22)$$

$$P_a = exp\left[-\frac{2}{\hbar}\int_{R_a}^{R_i}\left\{2\mu[V(R)-V(R_i)]\right\}^{\frac{1}{2}}\right]dR \quad (23)$$

$$P_b = exp\left[-\frac{2}{\hbar}\int_{R_i}^{R_b}\left\{2\mu[V(R)-Q]\right\}^{\frac{1}{2}}\right]dR \quad (24)$$

This means tunnelling starts at R = $R_a$ and ends at R = $R_b$, with $V_{Rb}$=Q value and between $P_i$ and $P_b$, the de-excitation probability ($W_i$) is assumed equal to unity [52]. Here, $R_a$ = $R_1$ +$R_2$ + ΔR is taken as the initial turning point. The relative separation distance ΔR between two fragments or clusters $A_i$ is supposed to account for the neck formation effects. The ΔR is used as a model parameter that is optimized in reference to available data.

The radius parameters used in Prox-77, Prox-88 and Prox BW-91 are mass dependent. However, the radii included in Prox-00 and Mod Prox-00 are A and Z dependent. Hence, the role of Z-dependent radius is also tested for Prox-77, Prox-88 and Prox BW-91 potentials which can be calculated through relation given by [40]:

$$R_i = 1.76Z_i^{1/3} - 0.96fm \quad (25)$$

## 3. Results and Discussions

The present investigation is dedicated to the ground state decay of Z=112-120 nuclear systems using the Preformed Cluster Model [7−12]. The work is divided into two sections: Section A comprises the decay analysis of heavy particle emission. Broadly saying, the investigation of heavy cluster radioactivity from Cn, Fl, Lv, Og and 120 isotopes is carried out by inculcating different proximity potentials namely Prox-77 [14], Prox-00 [15], Mod Prox-00 [16], Prox-88 [17], and Prox BW-91 [17] through the hot-deformed fragmentation approach. The ground state deformation effects are included upto $\beta_{2i}$. It is important to mention that the radii included in Prox-77, Prox-88, and Prox BW-91 potentials are mass number (A) dependent. Subsequently, proximity versions are modified by introducing Z-dependent radius parameters of the fragments given by Eq.(25). Using the mentioned cases of proximity potentials the decay half lives are calculated and compared with the estimates of [39]. Further, Sec B is designed to understand the spontaneous fission half-lives of Z=112-120 superheavy nuclei. Again various proximity potentials are tested by including A and Z dependent radii.

The cluster emission from the heavy and superheavy nuclei is explored to understand the ground state nuclear dynamics. In the heavy mass region, especially for the trans-lead nuclei the clusters such as $^{14}$C, $^{20}$O, $^{24}$Ne,$^{28}$Mg and $^{34}$Si are emitted corresponding to Pb-daughter nuclei. Fig. 1 is plotted to address the same for Fr-Cm nuclear systems. It is important to mention that the analysis of clusters in this mass region is primarily introduced to analyze the role of Prox-00 and Prox-77 potentials on cluster radioactivity so that the work can be extended to address the heavy cluster emission from superheavy mass region. Further, the decay half-lives of C-Si clusters are also ad-

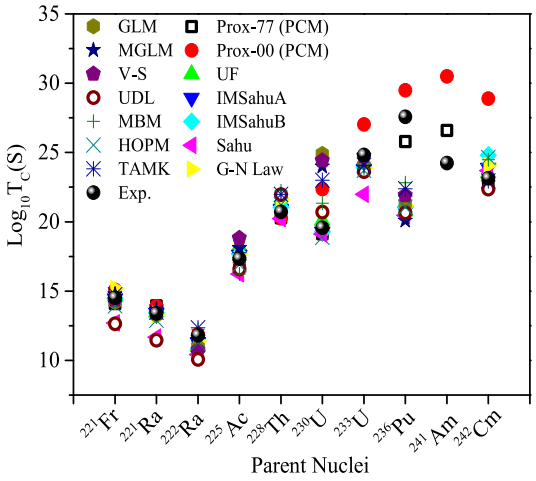


**Fig. 1.** (color online) Cluster decay half-lives plotted as a function of parent nuclei in trans-lead region. PCM based results of Prox-77 and Prox-00 proximity versions are presented and compared with experimental data along with the calculations of semi-empirical formulas [32, 53−57].

dressed in Ref. [11] of revised manuscript work with various proximity versions using the binding energies of [44]. However, the present cluster-analysis has been carried out for Audi and Wapstra's experimental binding energies [43]. It is clearly depicted from Fig. 1 that PCM calculated half-lives using Prox-77 and Prox-00 potentials show nice comparison with experimental estimates. The calculations with semi-empirical models [32, 53−57], show nice agrement with PCM based $\mathrm{Log}_{10}T_C$ data.

In the systematic search for nuclear decay modes the fragmentation profile of Z=112-120 nuclear systems is plotted in Fig. 2(a) as a function of light fragment mass ($A_2$). The fragmentation behavior is plotted for $^{282}$Cn, $^{284}$Fl, $^{292}$Lv,$^{294}$Og, and $^{300}$120 even-even nuclear systems for $\beta_{2i}$-hot deformed approach at best fitted neck-length parameters obtained for Prox-00. Hot orientations are considered at the lowest interaction radius corresponding to highest potential. It is clearly depicted from Fig. 1(a) that minima in the fragmentation potential are obtained at spontaneous fission and heavy cluster regions; hence considered as the prominent decay modes for Z=112-120 superheavy nuclei. Another striking observation that can be noted from this figure is that for $^{282}$Cn and $^{284}$Fl nuclear systems the minimum potential is noted for spontaneous fission region as compare to heavy cluster emission region. However as one moves towards heavier nuclei i.e. $^{292}$Lv,$^{294}$Og, and $^{300}$120, the minima in potential is observed in cluster region. This indicates that as we approaches towards heavier Z-nuclei, the possibility of heavy particle radioactivity increases as compare to spontaneous fission. This observation is in agrement with Ref. [5, 6]. Further, Fig. 2(b) is presented here just to check the role of different proximity potentials on the heavy particle emission and spontaneous fission processes. To account this study, $^{284}$Fl nucleus is taken into consideration. Interestingly, the emission of the $^{78}$Ge cluster remains intact with inclusion of different versions of proximity potentials. Moreover, the spontaneous fission region also remains same with Prox-77, Prox-00, Mod Prox-00, Prox-88 and Prox-BW-91 potentials.

The discussion of Fig. 2(a) signifies the dominance of heavy cluster emission and spontaneous fission decay modes. Following this, the mass distribution is plotted in

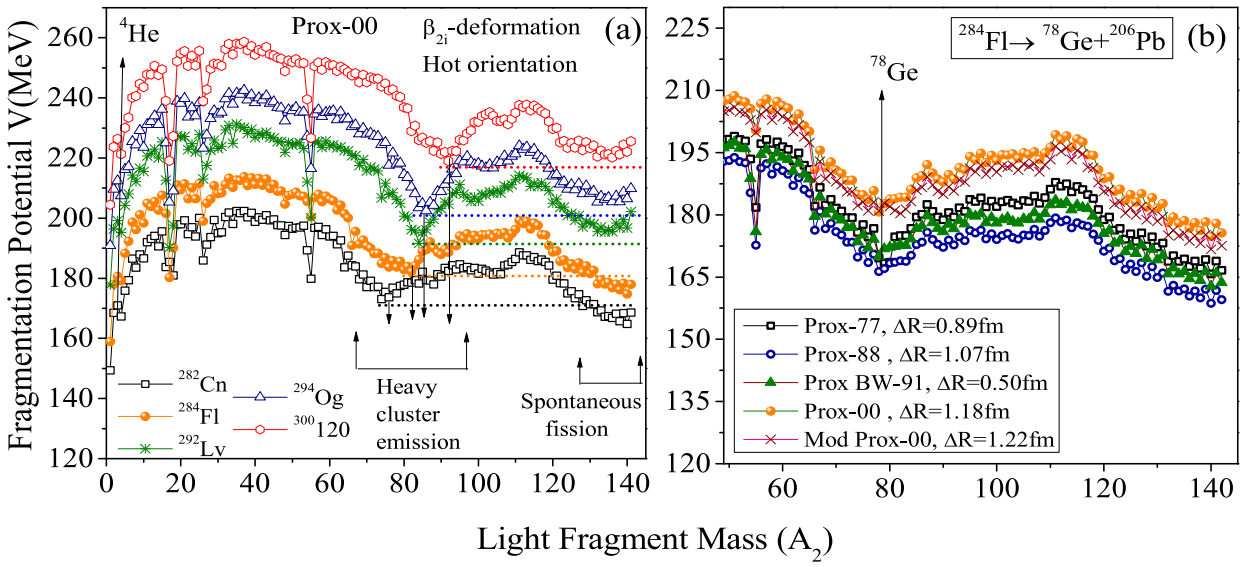


**Fig. 2.** (color online) Fragmentation potential plotted as a function of light fragment mass ($A_2$) for $^{282}$Cn, $^{284}$Fl, $^{292}$Lv,$^{294}$Og,$^{300}$120 even-even nuclear systems for Prox-00 potential. The regions of heavy cluster emission and spontaneous fission are mentioned in the plot. (b) is presented to check the effect of the different proximity potentials on decay path of superheavy nuclei; precisely the fragmentation of $^{284}$Fl is included here.

Fig. 3 to observe the decay trajectories of Z=112-120 superheavy nuclei. It is important to mention that the figure is presented for Prox-00 potential. It is clearly depicted from figures that the cluster emission is mainly governed through the Pb-nuclei which appears as the complementary fragment. Heavy cluster emission occurs via binary decay of HC (heavy cluster)+Pb (lead) fragments. This decay mode is purely associated with the shell effects of Pb nuclei. On the other hand, the spontaneous fission peaks are reinforced via highly deformed fission fragments. For the decay of Lv (Z=116), Og (Z=118), and Z=120 nuclear systems, the spontaneous fission decay is purely noted around asymmetric fragments having higher value of quadrupole deformations ($\beta_{2i}$) as mentioned in Fig. 3(c-e). Interestingly for Cn (Z=112) and Fl (Z=114) superheavy nuclei spontaneous fission is mostly observed around symmetric region (except for the heavier isotopes of Z=114) having octupole deformations ($\beta_{3i}$) (-0.054-(-0.136) for $^{144-148}$Ba and -0.042-(-0.128) for $^{144-148}$La) along with quadrupole one ($\beta_{2i}$) (see Fig. 3(a-b)). It is important to mention that the emergence of spontaneous fission region is shown at the neck-length parameters of heavy cluster emission to draw a comparative analysis. However, a complete discussion of spontaneous fission process is carried out in section 3.2.

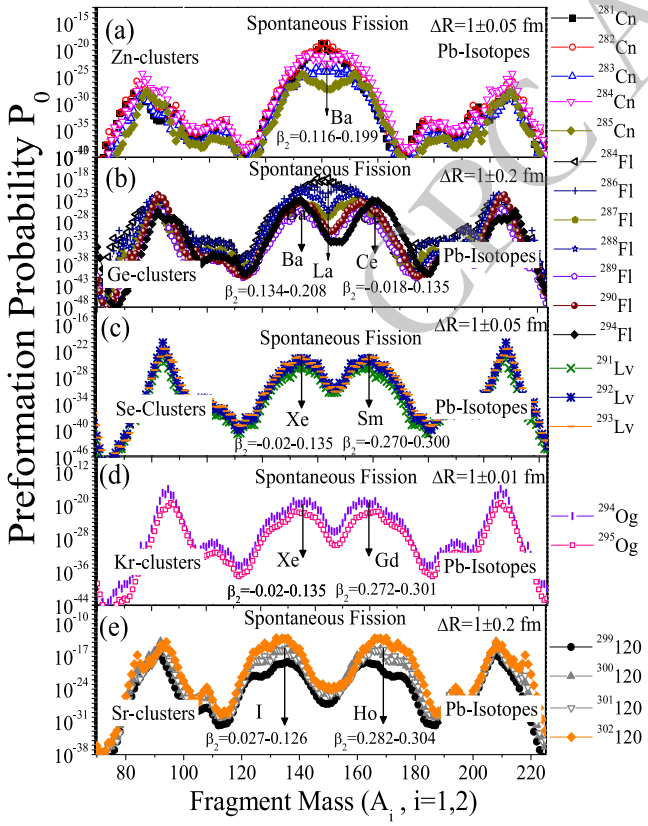


**Fig. 3.** (color online) Preformation Probability plotted as a function of fragment mass for investigating the decay modes of (a) Cn isotopes (b) Fl isotopes (c) Lv isotopes (d) Og isotopes (e) 120 isotopes using Prox-00 potential. The peaks of Pb-fragments can be clearly visualized. The spontaneous fission region is also shown in this figure for Z=112-120 superheavy nuclear systems.

### A. Heavy particle emission from Z=112-120 superheavy nuclei

In superheavy mass region with Z≥110 the heavier clusters $Z_e$>28 are observed along with doubly magic daughter $^{208}$Pb. To analyze the emitted heavy clusters the fragmentation potential is plotted for all the nuclei under consideration i.e. $^{281-285}$Cn, $^{284-294}$Fl, $^{291-293}$Lv, $^{294-295}$Og, and $^{299-302}$120 in Fig. 4. The figure clearly depicts that for Z=112 isotopes Zn clusters are emitted. Precisely, $^{73-74}$Zn are probable emitted clusters form $^{281,282}$Cn nuclei, whereas $^{283,284,285}$Cn systems expel $^{76}$Zn, $^{77}$Zn, and $^{78}$Zn clusters as shown in Fig. 4. In the similar manner $^{78,80-82,84}$Ge-clusters are emitted from $^{284-294}$Fl nuclear systems at the fixed values of the neck-length parameters in the range of 1±0.2 fm as shown in Fig. 4. Further Selenium ($^{84-85}$Se), Krypton ($^{84,86-88}$Kr) and Strontium ($^{91-94}$Sr) clusters are expected candidates emitted from Z=116 ($^{291-293}$Lv), Z=118 ($^{294-295}$Og) and Z=120 ($^{299-302}$120) nuclei respectively. The emitted clusters obtained from the potential minima are inline with the one as given by Poenaru *et al.* [39] along with some new clusters like $^{73}$Zn, $^{78}$Zn, $^{84}$Kr, and $^{88}$Kr.

Next, an attempt is made to address the heavy cluster decay half-lives ($Log_{10}T_C$) of Z=112-120 nuclear systems in reference to the ASAF data [39]. The cluster decay half-lives calculated in this work are the half-lives of the most probable emitted cluster which is in line with the one obtained from ASAF model. For this purpose Prox-77 [14] potential is used which is widely applied to address the the decay dynamics. The PCM calculated half-lives ($Log_{10}T_C$) for different isotopes are plotted in Fig. 5(a). For Prox-77 potential, the cluster decay half-lives of Z=112 and Z=114 isotopes are calculated within the estimates of ASAF calculations [39]. Unfortunately, the decay half-lives could not be addressed through Prox-77 for Z≥116. Apart from mentioned proximity potential, Prox BW-91 [17] is further included in calculations which is based on the Woods-Saxon parametrization concept. Prox BW-91 is the refined version of Prox CW-76 potential [46], hence instead of both, Prox BW-91 is inculcated for investigating the heavy cluster radioactivity. Again $^{281-285}$112 isotopes show nice comparison with ASAF measurements. However, some isotopes of Z=114 ($^{284-288}$114) can be addressed through BW-91 approach within the fixed range of ΔR~0.4-0.5 fm still not for Z≥116 nuclei as shown in Fig. 5(a). Next, Prox-88 [17] is included in the calculations which is modified version of Prox-77. With Prox-88 half-lives are harmonized with

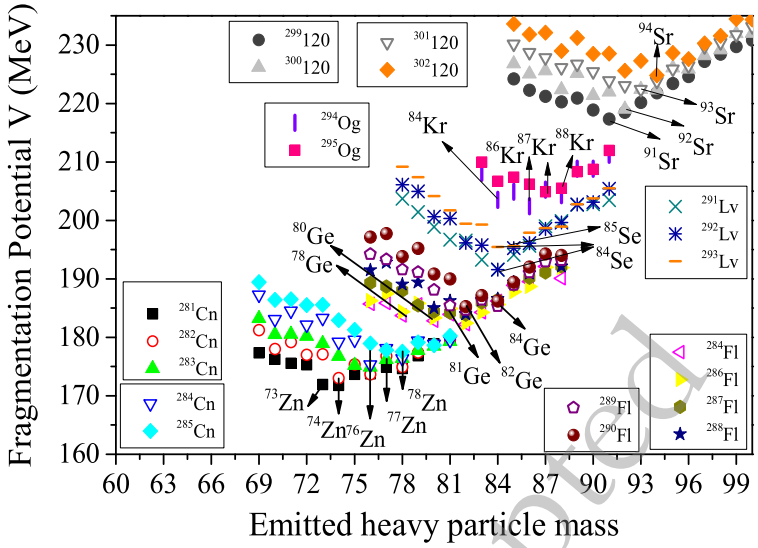


**Fig. 4.** (color online) Fragmentation potential plotted for heavy fragment mass region to analyze the emitted heavy clusters from different isotopes of superheavy nuclei in charge spectrum of Z=112-120.

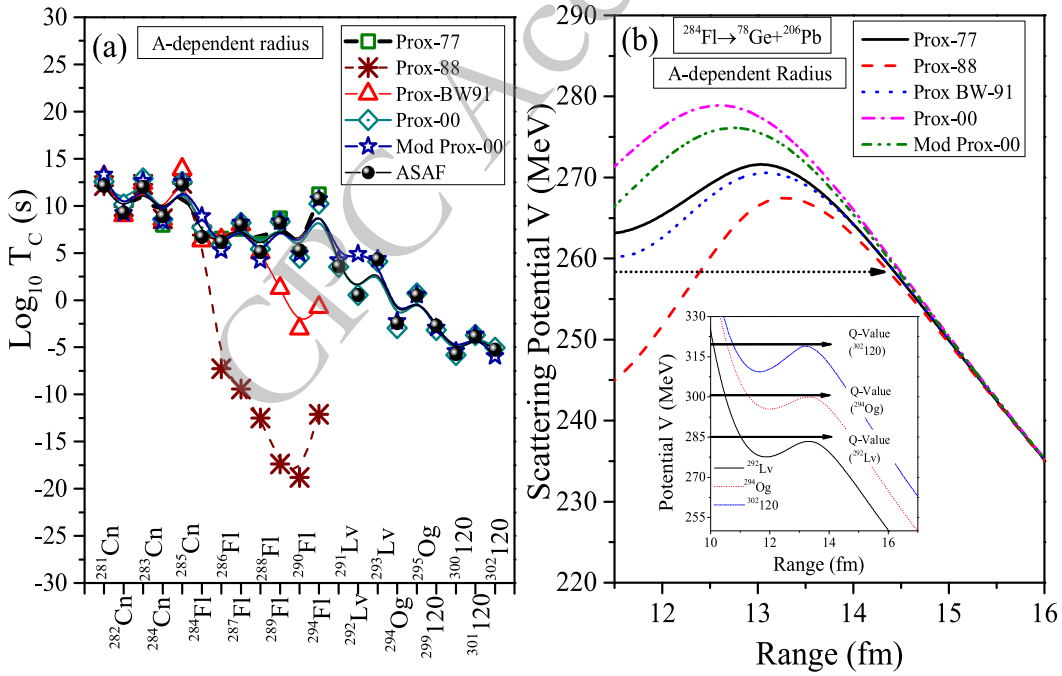


**Fig. 5.** (color online) (a) is plotted to compare the ASAF estimates of $Log_{10} T_C$ [39] with PCM calculated values. The A-dependent radii in different versions of proximity potentials are inculcated for calculating decay half-lives. (b) Variation of scattering potential V (MeV) as a function of internuclear radius or range R (fm) for the decay of $^{284}$Fl into $^{78}$Ge+$^{206}$Pb reaction with A-dependent radius parameters included for Prox-77, Prox-00, Mod Prox-00, Prox-88, and Prox-BW 91. The inset of Fig. 5(b) represents the scattering potential of Lv, Og and Z=120 with the inclusion of Prox-77 Potential.

ASAF data only for $^{281-285}$112 superheavy nuclei at ΔR~ 1.0 fm values. Lower magnitude of half-life values are obtained for Z=114 isotopes; finally $Log_{10} T_C$ of Z≥116 nuclei cannot be achieved within the application of Prox-88 potential as shown in Fig. 5(a). Conclusively, as the magnitude of potentials start decreasing from Prox-77 more nuclei start showing deviation from estimated cluster decay half-lives (see Fig. 5(b)). As lower potentials are not working well so Prox-00 [15], Mod Prox-00 [16] potentials are included in the calculations which have higher magnitude as compare to Prox-77, plotted in Fig. 5(b). The ASAF half-lives [39] are nicely addressed with Prox-00 and Mod Prox-00 potentials for all cases under consideration.

To further look into the matter, the scattering potential is plotted for $^{284}$Fl$\rightarrow$$^{78}$Ge+$^{206}$Pb reaction in Fig. 5(b) by introducing aforesaid proximity potentials. It is relevant to mention that $^{282-284}$Cn, $^{284-294}$Fl, $^{292}$Lv,$^{294}$Og, $^{300-302}$120 even-even nuclei and $^{281-285}$Cn, $^{287-289}$Fl, $^{293}$Lv, $^{295}$Og,$^{299-301}$120 even-odd nuclear systems are handled in the present analysis, but here Fig. 5(b) is plotted for $^{284}$Fl only as rest of the nuclei follow similar trend in scattering behavior. One can depict from this figure that highest potential is obtained for Prox-00 followed by Mod Prox-00, Prox-77, Prox BW-91 and Prox-88. Interestingly for Z=114 nuclear system the scattering potential is well above the Q-value (shown by doted horizontal arrow) for all proximity potentials and hence provide a suitable path for heavy cluster penetration. However, if one look at the inset of Fig. 5(b), which is plotted for Z=116,118, and 120 nuclei using Prox-77 potential, it is observed that the barrier height is quite lower than the Q-value for cluster emission and hence tunnelling is not possible. This justifies that the half-lives are not addressed for Z≥116 using Prox-77. Similar trend is followed for Prox-88 and Prox BW-91 potentials which is not shown here to avoid repetition. In order to rectify this, new set of binging energies prescribed by M. Wang *et. al.* [58] is introduced in the present analysis for two extreme nuclei under consideration i.e. $^{282}$Cn and $^{302}$120. Interestingly, same results are observed for both nuclei as mentioned earlier for Audi Wapstra's [43] case. Broadly speaking, the half-lives of Z=112 can be achieved with Prox-77 potential; however, $^{302}$120 nuclear system cannot be addressed through Prox-77 with new set of binging energies [58] too. In the similar manner, half-lives for Z=112 and Z=120 find nice agreement with ASAF measurements for Prox-00 potential as shown in Table 1. The Table is presented here to compare the results of Audi Wapstra's [43] with M. Wang [58] binding energies at same neck-length parameters for Prox-00 potential. It is clearly depicted from Table I that $Log_{10}T_c$ calculated for Z=112 and Z=120 isotopes are not varying much with both sets of binding energies. Further, the fragmentation potential for the same is shown in Fig. 6 and it is clear from figure that the structure of fragmentation potential remain same with minor variation in the magnitude. As the results in terms of decay half-lives and fragmentation potentials are nearly identical for both binging energies; hence, in the subsequent analysis Audi Wapstra's [43] binding energies are used.

The radius parameters of Prox-00 and Mod Prox-00 are mass number (A) and neutron excess (N-Z) dependent as shown by Eq.(12) and Eq.(14) respectively. However, the radii mentioned for Prox-77, Prox-88, and Prox BW-91 are exclusively mass number dependent. As matter density distribution of nucleus is different from proton density hence it will be of interest to include Z-dependent radius (see Eq.(25)) in these proximity potentials. This could be another alternative to address the $Log_{10}T_c$

**Table 1.** PCM calculated $Log_{10}$ $T_C$ for $^{282}$Cn and $^{302}$120 nuclei using Prox-00 potential with the help of G. Audi binding energy [43] and M. Wang binding energies [58]. ASAF calculated half-lives are also mentioned in table.

| Parent | Ref.[43] | | Ref.[58] | | ASAF [39] |
|---|---|---|---|---|---|
| | Q (MeV) | $Log_{10}T_C$ (Sec) | Q (MeV) | $Log_{10}T_C$ (Sec) | (Sec) |
| $^{282}$Cn | 244.46 | 10.15 | 246.3 | 9.01 | 9.29 |
| $^{302}$120 | 318.1 | −5.05 | 318.4 | −5.91 | −5.26 |

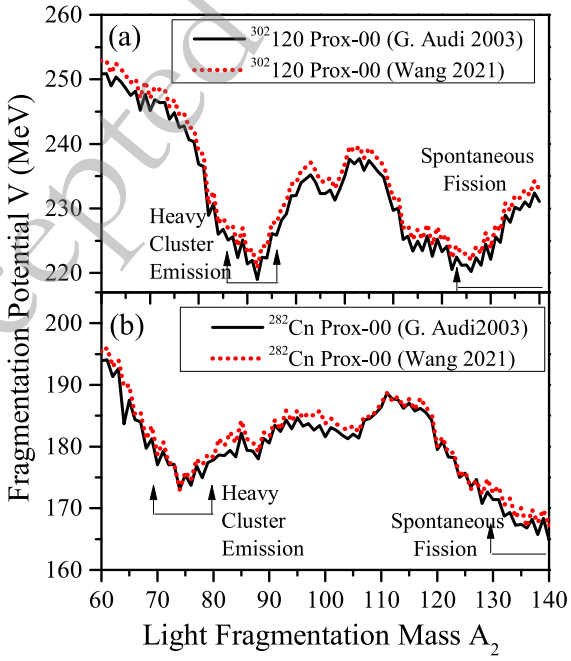


**Fig. 6.** (color online) Comparison of fragmentation potentials with the use of G. Audi binding energies [43] and M. Wang binding energies [58] for the decay of (a) $^{302}$120 and (b) $^{282}$Cn parent nuclei.

of Z≥116 nuclei instead of new set of binding energies. Fig. 7(a) is plotted to show the scattering behavior for Prox-77, Prox-88, Prox-00, and Prox BW-91 with Z-dependent radii. Fig. 7(a) clearly signifies that the magnitude of scattering potential is significantly uplifted with the inclusion of Z-dependant radius in Prox-77, Prox-88, and Prox BW-91 potentials.

For instance, the barrier height ($V_B$) in Fig. 5(b) for $^{284}$Fl is ~ 271 MeV which gets modified to 285 MeV by including the Z-dependent radius in Prox-77 potential. In the similar manner, the barrier height is 267 MeV and 279 MeV respectively for A-dependent and Z-dependent radius for Prox-88 for same nuclear system. The $V_B$ for Prox BW-91 is noted as 292 MeV for Z-dependant radius. The maximum change in the barrier height is measured for Prox-00 potential which is calculated at 311 MeV by replacing the Eq.(12) with exclusive Z-dependent case. It is relevant to mention that Eq.(25) dependent Prox-00 potential is discussed here simply to explore that

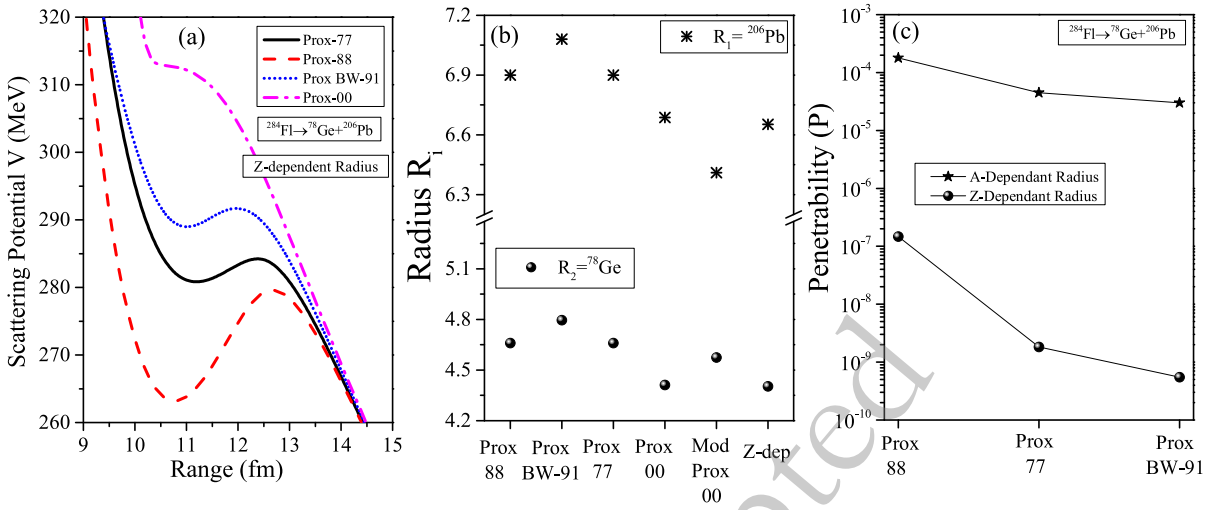


**Fig. 7.** (color online) (a) Variation of scattering potential V (MeV) as a function of internuclear radius or range R (fm) for Z-dependent radii in Prox-77, Prox-88, Prox-BW-91 and Prox-00 potentials. (b) shows the comparison of radius parameter with the use of A-dependent and Z-dependent equations. (c) is plotted to show the variation of the penetration probability for the same channel for Prox-77, Prox-88 and Prox BW-91 potentials with A and Z dependent radius parameters.

whether Z-dependent radius parameters work for this case or not. Interestingly, the pocket starts vanishing for this potential. Hence, the clear reason for not including Eq.(25) in Prox-00 is justified to address the dynamics of heavy cluster emission. The same is true for Mod Prox-00 potential. Further Fig. 7(b) is plotted for Prox-77, Prox-88, Prox BW-91, Prox-00, and Mod Prox-00 radius parameters, alongwith the Z-dependent radius given by Eq.(25). Interestingly, Z-dependant radius parameters are lower in magnitude than mass dependant radii for Prox-77, Prox-88, Prox BW-91; however, closer to the one obtained in Prox-00 case. The decrement in radius parameters becomes reason for enhancement in $V_B$ by including Z-dependence in radii and further show decrement in the barrier penetrability (see Fig. 7(c)) for the mentioned nuclear system. In this figure it is clearly seen that the penetration probability decreases for Eq.(25)-dependent radii. Hence, one may observe that the higher barrier height and lower penetration probability are required to address the cluster emission through Z-dependent radius as compared to A-dependent radius parameters.

By including the Z-dependent radii in Prox-77, Prox-88 and Prox-BW 91, better results can be visualized in Fig. 8(a) as compared to the previous case. The $Log_{10}T_C$ finds nice agreement with ASAF data for Z≥116 nuclei as well, depicted from the figure. Moreover, the neck-length parameters (ΔR) are also plotted in Fig. 8(b) for Z=112-120 nuclei for Z-dependant radius. It is clearly depicted from the figure that lower neck is required for the Z-dependent radii for calculating the half-lives as compared to A-dependent radius parameters for Prox-77, Prox-88 and Prox-BW 91 proximity potentials.

Fig. 9 is plotted to calculate the branching ratios of Z=112-118 superheavy nuclei. The branching ratio of cluster emission ($b_c$) relative to alpha decay can be calculated as:

$$Log_{10}(b_c) = Log_{10}(\lambda_c/\lambda_\alpha) = Log_{10}(T_\alpha/T_c) \qquad (26)$$

It is important to mention that the branching ratios are calculated only for those nuclear systems for which the experimental $\alpha$-decay half-lives are available. The chosen systems are mentioned in Fig. 9. For the calculations of alpha decay two proximity potentials are introduced namely Prox-00 and Prox-Ngô-80 in reference to the recent work [59]. The branching ratios show nice agreement with ASAF measurements (LiMaZe01 [19], KTUY05 [19] and W4 [39] mass tables) and Universal decay law (UDL) data [28] for Prox-00 potential for majority of nuclear systems. However, much higher $Log_{10}b_c$ values are calculated for $^{293}$Lv and $^{294}$Og nuclei. In order to rectify this, Ngô-80 proximity version [60] is introduced. The branching ratios for extreme nuclei (*i.e.* $^{293}$Lv and $^{294}$Og) decreases with Ngô-80 potential and nice comparison can be obtained with ASAF and UDL measurements. The $Log_{10}b_c$ of Santhosh *et.al.* [38] is also presented in Fig. 9 and compared with the calculated PCM values. The branching ratios with Prox-Ngô-80 potential show nice agrement with Santhosh *et.al.* data. However, lower branching ratios are reported with Universal (UNIV) curve [31], Unified description (UD) [32] estimates, and Scaling law of Horoi *et.al.* [33].

### B. Spontaneous Fission of Z=112-120 superheavy nuclei

In this section, the spontaneous fission half-lives of

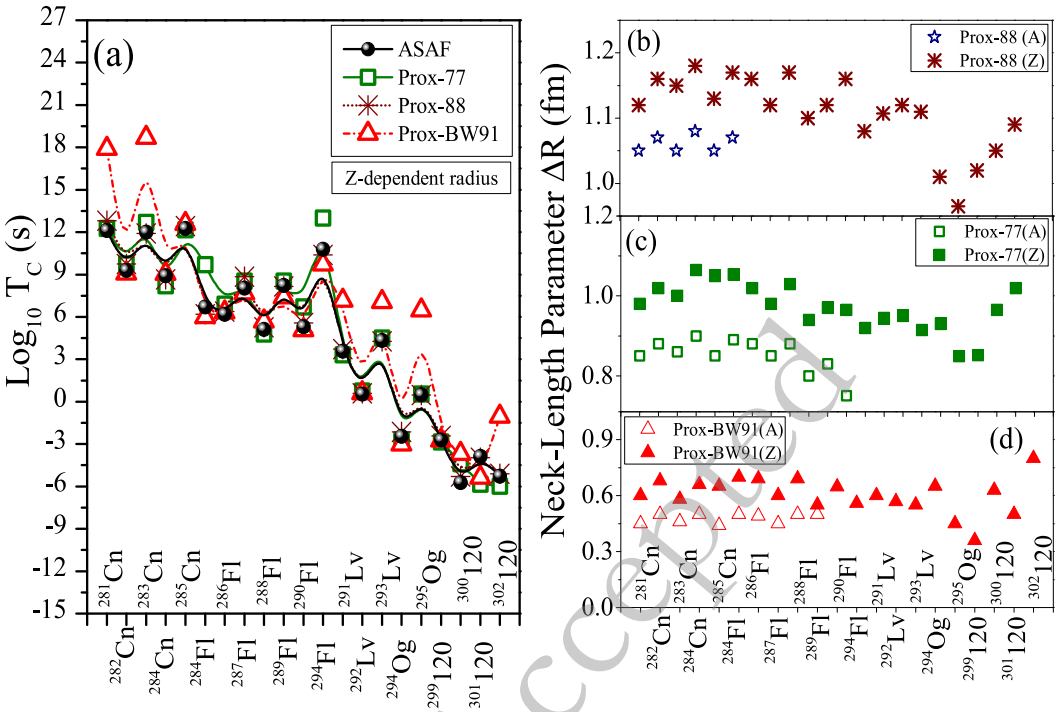


**Fig. 8.** (color online) (a) PCM calculated $\mathrm{Log}_{10}$ $T_C$ (sec) including Z-dependent radius parameters in Prox-77, Prox88 and Prox-BW 91 potentials. (b) Neck-length parameter variation for different proximities using A and Z-dependent radius parameters.

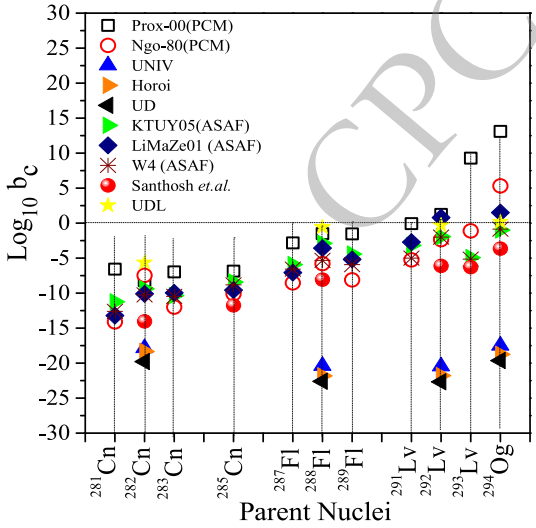


**Fig. 9.** (color online) Branching ratios are calculated using Prox-00 and Prox-Ngô-80 potentials. The results are compared with UNIV [31], Horoi [33], UD [32], UDL [28], ASAF with LiMaZe01 [19], KTUY05 [19] and W4 [39] mass tables. The measurements of Santhosh *et.al.* [38] are also shown in figure and compared with PCM fitted values.

$^{282,284}$Cn and $^{284,286}$Fl even-Z nuclear systems [61] are calculated by including different versions of proximity potentials same as in the previous section. Further the half-live predictions are carried out for Z=116-120 isotopes at different neck-length parameters. It is relevant to mention that even-even superheavy nuclei are taken into consideration because fission hindrance persists due to unpaired neutron or proton in even-odd and odd-odd nuclear systems. Firstly, the results for $^{282}$Cn, $^{284}$Cn, $^{284}$Fl and $^{286}$Fl nuclei are tabulated in Table 2 with the inclusion of Prox-00, Mod Prox-00, Prox-77 (A,Z), Prox-88 (Z) and Prox-BW-91 (Z) potentials. Here the half lives calculated through Prox-88 and Prox-BW-91 with A-dependent radii are not included which find the clarification in description of Fig. 10(a). The scattering potential in Fig. 10(a) signifies that the barrier height for Prox-88 (A) is lower than the Q-value for $^{138}$Ce+ $^{146}$Ba decay channel of $^{284}$Fl nuclear system. In the similar manner, Prox-BW-91 is also not appropriate to address the spontaneous fission of $^{284}$Fl nucleus as the barrier height approximately matches the Q-value of decay, hence difficult to achieve penetration of fission fragments through the barrier. On the other hand, other potentials mentioned in Fig. 10 seem to work for spontaneous fission process of superheavy nuclear system. Same results are true for $^{282,284}$Cn and $^{286}$Fl nuclear systems. Among the mentioned potentials, the spontaneous fission half-lives are overestimating the experimental data [61] upto much higher extent for Prox-77(Z) and Prox-BW 91 (Z) potentials. However, reasonably good comparison is obtained with the inclusion of Prox-77(A), Prox-00 and Mod Prox-00 potentials. The further investigation of Table 2 leads to a fact that Prox-00 and Prox-77 (A) give more appropriate results for Z=112 and Z=114 superheavy nuclei. However, the aim

**Table 2.** Comparison of PCM calculated spontaneous decay half lives ($T_c$) with experimental data [62] for Z=112 and 114 superheavy nuclei by including Prox-77 (A,Z), Prox-88 (Z), Prox BW-91(Z), Prox-00, Mod Prox 00 proximity potentials.

| Nucleus | $T_{SF}^{Expt.}$ | Prox-77(A) | | Prox-77(Z) | | Prox-00 | | Mod Prox-00 | | Prox-88 (Z) | | Prox BW-91(Z) | |
|---|---|---|---|---|---|---|---|---|---|---|---|---|---|
| | (ms) | $\Delta R$ (fm) | $T_{SF}$ (ms) | $\Delta R$ (fm) | $T_{SF}$ (ms) | $\Delta R$ (fm) | $T_{SF}$ (ms) | $\Delta R$ (fm) | $T_{SF}$ (ms) | $\Delta R$ (fm) | $T_{SF}$ (ms) | $\Delta R$ (fm) | $T_{SF}$ (ms) |
| $^{282}$Cn | 0.91 | 0.946 | 0.98 | 0.959 | $1.09\times10^{5}$ | 1.075 | 1.6 | 1.110 | 1.5 | 1.214 | 12.9 | 0.65 | $3.2\times10^{6}$ |
| $^{284}$Cn | 98 | 0.945 | 84.8 | 0.972 | $1.15\times10^{6}$ | 1.075 | 76.9 | 1.109 | 29.9 | 1.220 | 0.18 | 0.65 | $5.1\times10^{8}$ |
| $^{284}$Fl | 2.5 | 0.894 | 2.06 | 0.940 | $1.63\times10^{2}$ | 1.005 | 1.6 | 1.111 | 11.6 | 1.173 | 3.50 | 0.62 | $8.38\times10^{5}$ |
| $^{286}$Fl | 120 | 0.950 | 0.55 | 0.956 | $1.9\times10^{5}$ | 1.035 | 150 | 1.074 | 264 | 1.197 | 134 | 0.62 | $2.95\times10^{8}$ |

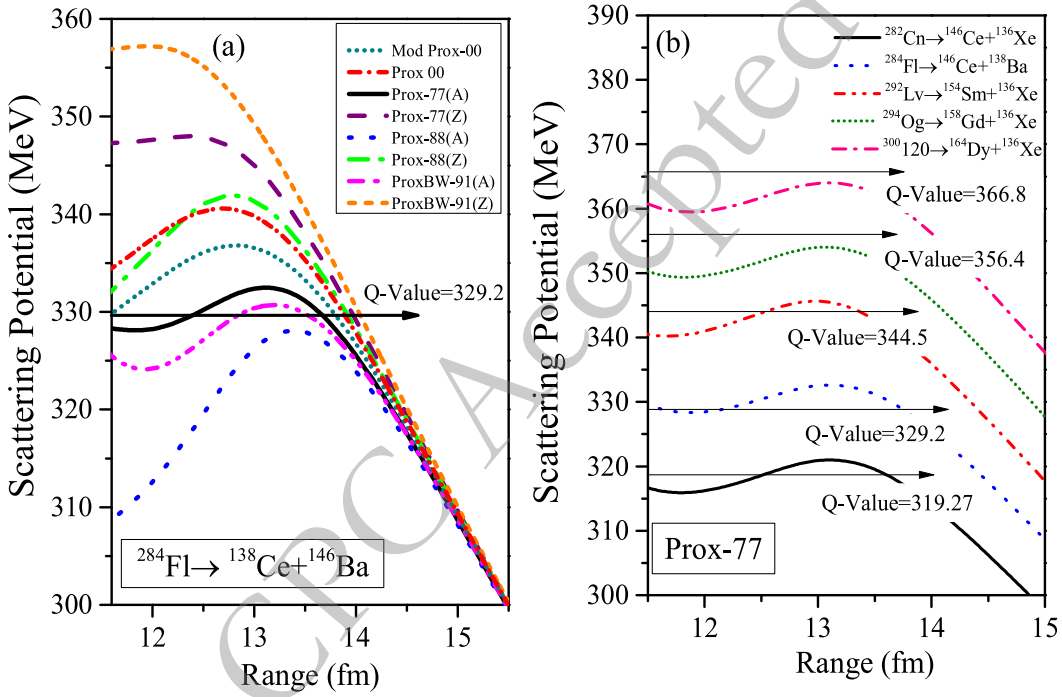




**Fig. 10.** (color online) (a) Scattering potential plotted as a function of interaction range for the fission channel emitted from $^{284}$Fl nuclear system using various versions of proximity potentials.(b) Scattering potentials for Z=112-116 superheavy nuclei with the inclusion of Prox-77 potential.

of the present analysis is to choose the best version of proximity potential to address the spontaneous fission process. Owing to this, Fig. 10(b) is plotted which clarifies that the Prox-77 (A) can be applied to Z≤116 nuclear systems ($^{284}$Fl and $^{282}$Cn) because for higher superheavy systems the Q-value overestimates the barrier height. Hence Prox-00 is the best proximity version to handle spontaneous fission half-lives for superheavy mass region.

Conclusively, Prox-00 is the most probable proximity version which can handle the ground state emission such as heavy particle radioactivity and spontaneous fission simultaneously. Moreover, the Z-dependence in the proximity potentials work well only for the heavy particle emission and not appropriate to address the spontaneous fission half lives of superheavy nuclei. Owing to this, the spontaneous fission half-lives are calculated using Prox-00 potential at different neck-length parameters ranging 1 fm-1.1 fm in Fig. 11 for $^{292}$Lv, $^{294}$Og, $^{300,302}$120 nuclei which could provide a testing ground for the future experiments on spontaneous fission. Fig. 11 signifies that the fission half-lives show decrement with increase in neck-length parameters.

Finally, the total kinetic energy (TKE) is calculated for Z=112-120 nuclei by introducing Coulomb and Proximity potentials at the scission point of the barrier. The Q (value)= TKE+TXE, where TKE is total kinetic energy of the decay fragments and TXE corresponds to total excitation energy. Since the parent and daughter nuclei are considered in ground state hence the Q~ TKE. Fig. 12 is plotted to observe the calculated TKE alongwith the experimental [62] and theoretical estimates of [63−65]. It is observed that the PCM calculated TKE magnitudes lie in the range of 320-365 MeV, which are quite higher than the experimental values. Hence, the formula for calculating TKE values is again revisited and a factor of 0.7 is in-

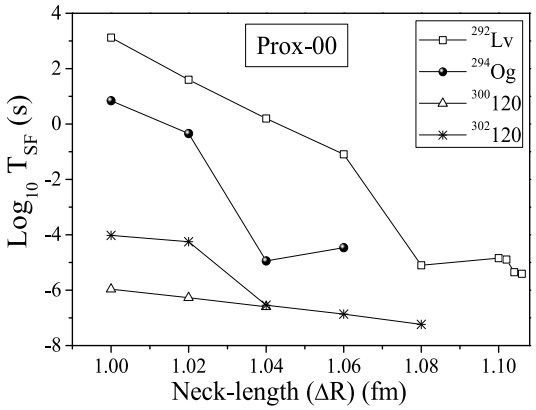


**Fig. 11.** (color online) Spontaneous fission half-lives calculated using Prox-00 potential for $^{292}$Lv $^{294}$Og, $^{300}$120 and $^{302}$120 superheavy nuclei.

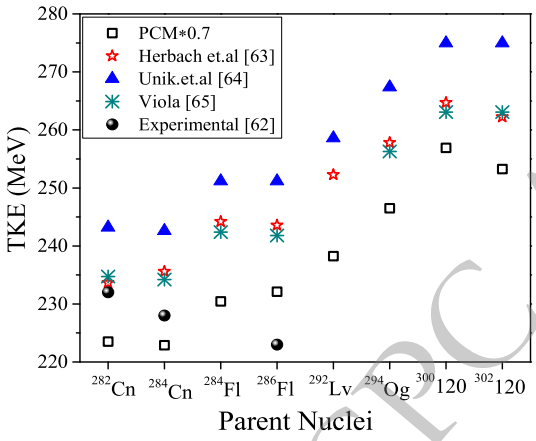


**Fig. 12.** (color online) PCM calculated TKE-values for Z=112-120 superheavy nuclei alongwith the formulae given by [63−65]. The estimated values are compared with the experimental TKE data [62].

troduced while calculating the $V_C$ and $V_P$ at scission point of fission fragments of $^{282}$Cn, $^{284}$Cn, $^{284}$Fl, $^{286}$Fl, $^{292}$Lv, $^{294}$Og, $^{300}$120 and $^{302}$120 nuclear systems. The formula for estimating TKE given by [63] finds nice agreement with experimental TKE data [62]. This formula is fabricated by introducing the modified version of Coulomb potential (see Ref([63]), hence it is justified that the traditional expression of Coulomb potential needs modification for addressal of TKE-values. The same argument is considered for TKE-calculation for binary fragmentation in Unik *et.al* [64] and Viola systematics [65]. Both fit the experimental data nicely. Owing to this, the Coulomb and proximity potentials in PCM are modified to attain the experimental TKE-values, which are now calculated as $(V_C+V_P)\times0.7$ to acquire the experimental TKE-values. It is relevant to mention that $(V_C+V_P)\times0.65$ is used for temperature dependent case, where the emission from the hot and rotating compound nucleus is included [66].

## IV. SUMMARY

The heavy particle radioactivity and spontaneous fission phenomenon are addressed through the Preformed Cluster Model (PCM) for Z=112-120 (even-Z) superheavy nuclei. The fragmentation structure reveal that upto Z=114 there are higher chances of spontaneous fission whereas heavy particle radioactivity starts competing for heavier superheavy nuclei (Z>114). Also the preformation structure shows that the heavy clusters are primarily governed through magic shell effects whereas spontaneous fission is reinforced by the higher order deformations of the decaying fission fragments. The cluster decay half lives are worked out via Prox-77, Prox-88, Prox-BW-91, Prox-00 and Mod Prox-00 proximity potentials using A-dependant radius. However, the Z-dependent radius parameter is used to find the corresponding barrier characteristics, potentials and decay half-lives, and a comparison is made with A-dependant case. Higher barrier height, neck-length parameter (ΔR) and lower penetrability is observed for Z-dependent case as compared to A-dependent radius parameter used in different proximity potentials. The branching ratios are also calculated through Prox-00 and Prox Ngô-80 potentials and compared with UNIV, UD, Horoi, and ASAF measurements. The Log$_{10}$(b$_c$) are also compared with Santhosh *et. al.*. Nice comparison with Prox Ngô-80 is obtained for Z=112-118 superheavy nuclei. Further, the cluster decay and spontaneous fission half-lives of nuclei upto Z≤114 are in the decent agrement with ASAF data using Prox-77(A). Whereas for heavier nuclei (Z>114), Prox-00 ($T_C$, $T_{SF}$), Mod Prox-00 ($T_C$, $T_{SF}$), and Prox-77(Z)($T_C$) seems to provide better option for the addresal of half-lives. Finally, the TKE-values are calculated and compared with experimental data.



## References


[1] O. Hahn, F. Strassman, Naturwissenschaften **27**, 11 (1939)

[2] A. Sobiczewski, F. A Gareev, B. N Kalinkin, Phys. Lett. **22**, 500 (1996)

[3] H. Meldner, Ark. Fys., **36**, 593 (1967); S. G. Nilsson, J. R. Nix, A. Sobiczewski, Z. Szymanski, S. Wycech, C. Gustafson and P. Mo11er, Nucl. Phys. A, **545**: ll5 (1968).

[4] Yu. Ts. Oganessian *et. al.*, Phys. Rev. Lett., **108**: 022502 (2012); Phys. Rev. C, **87**: 014302 (2013); Yu. Ts. Oganessian *et. al.*, Phys. Rev. C, **83**: 054315 (2011).

[5] G. G. Adamian et. al., Eur. Phys. J. A **57**, 89 (2021)

[6] F.P. Heßberger, Eur. Phys. J. A **53**, 75 (2017)

[7] R. K. Gupta, in Proceedings of the 5th International Conference on Nuclear Reaction Mechanisms, edited by E.

Gadioli (Ricerca Scientifica ed Educazione Permanente, Milan, 1988), p. 416.
[8] S. S. Malik and R. K. Gupta, Phys. Rev. C **39**, 1992 (1989)
[9] S. Kumar and R. K. Gupta, Phys. Rev. C, **55**: 218 (1997); S. Kumar, M. Balasubramaniam, R. K. Gupta, G. Münzenberg, W. Scheid, J. Phys. G: Nucl. Part. Phys., **29**: 625 (2003).
[10] G. Sawhney, M. K. Sharma, and R. K. Gupta, Phys. Rev. C **83**, 064610 (2011)
[11] R. Kumar, Phys. Rev. C **86**, 044612 (2012)
[12] G. Sawhney, K. Sandhu, M. K. Sharma and R. K. Gupta Eur, Phys. J. A **50**, 175 (2014)
[13] R. K. Gupta, M. Balasubramaniam, R. Kumar, N. Singh, M. Manhas, and W. Greiner, J. Phys. G **31**, 631 (2005)
[14] J. Blocki, J. Randrup, W. J. Swiatecki, and C. F. Tsang, Ann. Phys. (NY) **105**, 427 (1977)
[15] W. D. Myers and W. J. Swiatecki, Phys. Rev. C **62**, 044610 (2000)
[16] G. Royer and R. Rousseau, Eur. Phys. J. A **42**, 541 (2009)
[17] W. Reisdorf, J. Phys. G: Nucl. Part. Phys. **20**, 1297 (1994)
[18] D. N. Poenaru, R. A. Gherghescu, W. Greiner, Phys. Rev. Lett. **107**, 062503 (2011)
[19] D. N. Poenaru, R. A. Gherghescu, W. Greiner, Phys. Rev. C **85**, 034615 (2012)
[20] R. Bonetti and A. Guglielmetti, Rom. Rep. Phys., **59**: 301 (2007); R. Bonetti, C. Carbonini, A. Guglielmetti, M. Hussonnois, D. Trubert, and C. Le Naour, Nucl. Phys. A, **686**: 64-70 (2001).
[21] P. B. Price, Annu. Rev. Nucl. Part. Sci. **39**, 19 (1989)
[22] D. N. Poenaru, Y. Nagame, R. A. Gherghescu, and W. Greiner, Phys. Rev. C **65**, 054308 (2002)
[23] D. N. Poenaru, M. Ivascu, A. Sandulescu, and W. Greiner, Phys. Rev. C **32**, 572 (1985). D. N. Poenaru, W. Greiner, K. Depta, M. Ivascu, D. Mazilu, and A. Sandulescu, At. Data Nucl. Data Tables, **34**: 423 (1986).
[24] Y. J. Shi and W. J. Swiatecki, Phys. Rev. Lett. **54**, 300 (1985)
[25] G. A. Pik-Pichak, Fiz. Elem. Chastits At. Yadra, **44**: 1421 (1986)[Sov. J. Part. Nucl., **44**: 923 (1986)].
[26] G. Royer and R. Moustabchir Nucl. Phys. A., **683**: 182 (2001); G. Royer Phys. J. Phys. G Nucl. Part. Phys., **26**: 1149 (2000); G. Royer and R. A. Gherghescu Nucl. Phys. A, **699**: 479 (2002).
[27] A. M. Nagaraja et. al., Nucl. Phys. A **1015**, 122306 (2021)
[28] C. Qi, F. R. Xu, R. J. Liotta, and R. Wyss, Phys. Rev. Lett. **103**, 072501 (2009)
[29] M. Ismail and A. Adel, J. Phys. G: Nucl. Part. Phys. **49**, 075102 (2022)
[30] A. Adel and T. Alharbi, Nucl. Phys. A **958**, 187 (2017)
[31] D. N. Poenaru, R. A. Gherghescu, and W. Greiner, Phys. Rev. C **83**, 014601 (2011)
[32] D. D. Ni, Z. Z. Ren, T. K. Dong, and C. Xu, Phys. Rev. C **78**, 044310 (2008)
[33] M. Horoi, B. A. Brown, and A. Sandulescu, J. Phys. G: Nucl. Part. Phys. **30**, 945 (2004)
[34] D. T. Akrawy, and D. N. Poenaru, J. Phys. G: Nucl. Part. Phys. **44**, 22001 (2017)
[35] R. Blendowske and H. Walliser, Phys. Rev. Lett. **61**, 1930 (1988)
[36] Z. Ren, C. Xu, and Z. Wang, Phys. Rev. C, **70**: 034304 (2004); D. Ni and Z. Ren, Phys. Rev. C, **82**: 024311 (2010).
[37] B. B. Singh, S. K. Patra, and R. K. Gupta, Phys. Rev. C, **82**: 014607 (2010); Int. J. Mod. Phys. E, **20**: 1003 (2011).
[38] K. P. Santhosh and C. Nithya, Phys. Rev. C **97**, 064616 (2018)
[39] D. N. Poenaru, H. Stocker, and R. A. Gherghescu, Eur. Phys. J. A **54**, 14 (2018)
[40] L. C. Chamon et. al., Phys. Rev. C **70**, 014604 (2004)
[41] J. Maruhn and W. Greiner, Phys. Rev. Lett. **32**, 548 (1974)
[42] R. K. Gupta, W. Schied, and W. Greiner, Phys. Rev. Lett. **35**, 353 (1975)
[43] G. -Audi, A. H. Wapstra and C. Thibault, Nucl. Phys. A **729**, 337 (2003)
[44] P. Möller, J. R. Nix, W. D. Myers, and W. J. Swiatecki, At. Data Nucl. Data Tables **59**, 185 (1995)
[45] W. Myers and W. J. Swiatecki, Nucl. Phys. **81**, 1 (1966)
[46] I. Dutt and R.K. Puri, Phys. Rev. C **81**, 064609 (2010)
[47] C. Y. Wong *et al*., Phys. Rev. Lett. **31**, 766 (1973)
[48] K. Alder and A. Winther, Nucl. Phys. A **132**, 1 (1969)
[49] V. Yu. Denisov, Phys. Rev. C **88**, 044608 (2013)
[50] M. Mirea, A. Sandulescu, D. S. Delion, Eur. Phys. J A. **48**, 86 (2012)
[51] H. Kröger and W. Scheid, J. Phys. G: Nucl. Phys. **6**, L85 (1980)
[52] M. Greiner and W. Scheid, J. Phys. G: Nucl. Part. Phys. **12**, L229 (1986)
[53] Y. Wang, F. Xing, Y. Xiao, and J. Gu, Chinese Phys. C **45**, 044111 (2021)
[54] X. Y. Zhu et. al., Chinese Phys. C **47**, 114103 (2023)
[55] A. V. Afanasjev and S. Frauendrof, Phys. Rev. C **71**, 024308 (2005)
[56] H. M. Liu et. al., Phys. Scr. **96**, 125322 (2021)
[57] J. Qi et. al., Chinese Phys. C **47**, 064107 (2023)
[58] M. Wang et. al., Chinese Phys. C **45**, 030003 (2021)
[59] K. Sharma and M. K. Sharma, Nucl. Phys. A **986**, 1 (2019)
[60] H. Ngo and C. Ngô, Nucl. Phys. A **348**, 140 (1980)
[61] Yu. Oganessian, and V.K. Utyonkov, Nuclear Physics A **944**, 62 (2015)
[62] Yu. Oganessian, J. Phys. G: Nucl. Part. Phys. **34**, R165 (2007)
[63] C.-M. Herbach et.al., Nuclear Physics A **712**, 207 (2002)
[64] J.P. Unik, J.E. Gindler, L.E. Glendenin, K.F. Flynn, A. Gorski, R.K. Sjoblom, in Proceedings of the IAEA Symposium "Physics and Chemistry of Fission", Rochester, New York, August 13-17, 1973 Vol. II (IAEA, Vienna, 1974) p. 19 ff.
[65] V.E. Viola jr., K. Kwiatkowski, M. Walker, Phys. Rev. C **31**, 1550 (1985)
[66] Gurjit Kaur, K. Sandhu, M. K. Sharma, Phys. Rev. C **94**, 014615 (2016)